Behavior of rotating magnetic microrobots above the step-out frequency with application to control of multi-microrobot systems

Arthur W. Mahoney,[1] Nathan D. Nelson,[2] Kathrin E. Peyer,[3] Bradley J. Nelson,[3] and Jake J. Abbott[2]
[1]*School of Computing, University of Utah, Salt Lake City, Utah 84112, USA*
[2]*Department of Mechanical Engineering, University of Utah, Salt Lake City, Utah 84112, USA*
[3]*Institute of Robotics and Intelligent Systems, ETH Zurich, CH-8092 Zurich, Switzerland*

(Received 7 March 2014; accepted 26 March 2014; published online 7 April 2014)

This paper studies the behavior of rotating magnetic microrobots, constructed with a permanent magnet or a soft ferromagnet, when the applied magnetic field rotates faster than a microrobot's step-out frequency (the frequency requiring the entire available magnetic torque to maintain synchronous rotation). A microrobot's velocity dramatically declines when operated above the step-out frequency. As a result, it has generally been assumed that microrobots should be operated beneath their step-out frequency. In this paper, we report and demonstrate properties of a microrobot's behavior above the step-out frequency that will be useful for the design and control of multi-microrobot systems. © *2014 AIP Publishing LLC*. [http://dx.doi.org/10.1063/1.4870768]

Untethered magnetic microrobots show promise for a variety of applications including minimally invasive medicine[1] and manipulation.[2] Magnetic microrobots are generally simple devices actuated by externally applied magnetic fields that exert some combination of magnetic force and torque upon the microrobot.

This paper studies microrobots whose primary form of locomotion converts magnetic torque into propulsion using a continuously rotating magnetic field. This includes microrobots that roll or propel via an attached rigid chiral structure (e.g., a helix or screw). When the applied magnetic field rotates sufficiently slowly, the microrobots synchronously rotate with the field. There exists a field rotation frequency, however, above which the applied magnetic torque is not strong enough to keep the microrobot synchronized with the field. This frequency is the "step-out" frequency.[3] The step-out frequency depends on the microrobot's magnetization, friction, and the field strength. When operated above the step-out frequency, the microrobot's velocity rapidly declines.

The ability to control multi-microrobot systems is desirable for manipulation applications.[2] Most existing multi-microrobot systems are actuated by uniform magnetic fields where each microrobot experiences the same actuating signal, making true independent control difficult. Control methods for multi-microrobot systems exist when each microrobot responds differently to the actuating signal.[4] Common techniques include designing each microrobot to convert a rotating magnetic field into spatial motion at different rates, and varying the step-out frequency between microrobots so that one loses synchronization with the rotating field before another, enabling semi-selective binary control.[3] In this paper, we present properties of a microrobot's decline in velocity, above step-out, that enables the velocity of individuals in a multi-microrobot system to be designed to selectively respond uniformly to the rotating field (where the microrobot rotation velocities are the same), respond heterogeneously where some microrobots have lost synchronization and others have not (where the ratio of the microrobot rotation velocities is large as demonstrated by Ishiyama *et al.*[3]), or respond heterogeneously with all microrobots having lost synchronization (where the ratio of the microrobot rotation velocities approaches a pre-designed constant). The phenomenon we present can be exploited by control-theoretic techniques,[4] or it can add an additional level of microrobot differentiation to existing multi-microrobot control strategies such as addressable microrobot methods, which have been demonstrated to be well-suited for positioning and manipulation tasks.[2]

When a microrobot with dipole moment $\mathbf{m} \in \mathbb{R}^3\,\mathrm{A\,m^2}$ is placed in a magnetic field $\mathbf{h} \in \mathbb{R}^3\,\mathrm{A/m}$, a magnetic torque $\boldsymbol{\tau}_\mathbf{h} = \mu_0 \mathbf{m} \times \mathbf{h}$ will be applied, where $\mu_0 = 4\pi \times 10^{-7}\,\mathrm{T\,m/A}$. For a permanent-magnet microrobot, the dipole moment is fixed with respect to the microrobot's geometry. For a microrobot with a soft-magnetic body of volume v that can be approximated as an ellipsoid, the dipole moment varies with the applied magnetic field according to $\mathbf{m} \approx v\mathcal{X}\mathbf{h}$, where $\mathcal{X} \in \mathbb{R}^{3\times3}$ is the apparent susceptibility matrix. When expressed in a coordinate system with axes aligned to the principal directions of the approximating ellipsoid, then $\mathcal{X}$ can take on the form

$$\mathcal{X} = \mathrm{diag}\left(\frac{\chi}{1+n_a\chi}, \frac{\chi}{1+n_r\chi}, \frac{\chi}{1+n_r\chi}\right), \tag{1}$$

where n_a and n_r are the demagnetization factors in the directions of the major and minor ellipse axes (so that $n_a < n_r$), respectively, and χ is the susceptibility of the material.[5] When the applied magnetic fields are sufficiently strong, then the moment becomes saturated so that $\|\mathbf{m}\| = m_{\mathrm{sat}}$ and $\mathbf{m}$ aligns to minimize the total magnetic energy. Let h_{sat} be the field magnitude required to saturate the microrobot's magnetic body.

In this paper, we assume a simple 1-degree-of-freedom (DOF) model where the magnetic microrobot's angular velocity $\boldsymbol{\omega}_\mathbf{m} \in \mathbb{R}^3\,\mathrm{rad/s}$ and the applied magnetic torque $\boldsymbol{\tau}_\mathbf{h}$ are parallel to the microrobot's principal axis, and the microrobot's dipole moment $\mathbf{m}$ and the applied field $\mathbf{h}$ are perpendicular to,

and rotate around, the same principal axis (see Fig. 1). The magnetic field's angular velocity is denoted as $\boldsymbol{\omega}_\mathbf{h} \in \mathbb{R}^3$ rad/s, which we assume to be constant. In low-Reynolds-number regimes, a microrobot's spatial velocity is generally assumed to be proportional to its rotational frequency. The magnitudes of the magnetic torque, the microrobot's angular velocity, and the magnetic field's angular velocity are denoted by τ_h, ω_m, and ω_h, respectively. Although the 1-DOF assumption is not true in general for helical microrobots, whose chiral asymmetry causes precession particularly at slow rotation speeds, the model tends to be a good approximation.

We also assume the applied magnetic field is uniform (i.e., no magnetic force is applied) and the microrobot operates in low-Reynolds-number regime fluids, where inertia is negligible and the microrobot's angular velocity is proportional to the applied magnetic torque by a viscous drag coefficient c, which varies with surface friction, fluid viscosity, and microrobot geometry. Under these assumptions, a permanent- and soft-magnetic microrobot's angular velocity can be modeled as

$$\omega_\mathrm{m} = \frac{1}{c}\tau_\mathrm{h} = \begin{cases} \omega_\mathrm{so}\sin(\alpha), & \text{permanent magnet} \\ \omega_\mathrm{so}\sin(2\alpha), & \text{soft magnet,} \end{cases} \tag{2}$$

where α is the angle illustrated in Fig. 1. The soft-magnetic microrobot's angular velocity in (2) is accurate when either well below or above saturation.[5] The scalar ω_so is the maximum angular velocity achievable (when τ_h is maximized at $\alpha = \pi/2$ rad and $\alpha = \pi/4$ rad for a permanent- and soft-magnetic microrobot, respectively).

For a permanent magnet, the step-out frequency is

$$\omega_\mathrm{so} = \mu_0\|\mathbf{m}\|\|\mathbf{h}\|/c, \tag{3}$$

which is linear with $\|\mathbf{h}\|$ and the microrobot's dipole moment $\|\mathbf{m}\|$, which depends on the remanent magnetization and volume v of the magnetic body.

The step-out frequency of a soft-magnetic microrobot changes between the magnetic saturation regimes and is

$$\omega_\mathrm{so} = \begin{cases} \dfrac{\mu_0}{c}\dfrac{|n_a - n_r|}{2n_a n_r} v\|\mathbf{h}\|^2, & \text{when } \|\mathbf{h}\| \ll h_\mathrm{sat} \\ \dfrac{\mu_0}{c}\dfrac{|n_a - n_r|}{2} v m_\mathrm{sat}^2, & \text{when } \|\mathbf{h}\| \geq h_\mathrm{sat}, \end{cases} \tag{4}$$

which increases quadratically with $\|\mathbf{h}\|$ below saturation, but is limited by the saturated moment m_sat of the magnetic body above saturation. The step-out frequency varies with the soft-magnetic body's geometry through the demagnetization factors, n_a and n_r, and is proportional to the soft-magnetic body's volume v. Between the two magnetization regimes, the step-out frequency falls between the frequencies given in (4).

The *average* microrobot angular velocity $\bar{\omega}_\mathrm{m}$, as a function of the field rotating frequency ω_h, has been solved in closed-form for both rotating permanent magnets[6–8] and ferromagnetic ellipsoids.[9] In both cases, $\bar{\omega}_\mathrm{m}$ is found as

$$\bar{\omega}_\mathrm{m} = \begin{cases} \omega_\mathrm{h}, & \text{when } \omega_\mathrm{h} \leq \omega_\mathrm{so} \\ \omega_\mathrm{h} - \omega_\mathrm{h}\sqrt{1 - (\omega_\mathrm{so}/\omega_\mathrm{h})^2}, & \text{when } \omega_\mathrm{h} > \omega_\mathrm{so}. \end{cases} \tag{5}$$

Equation (5) can be used to study the effects of scaling an individual microrobot's step-out frequency or the comparative difference between microrobots in a group with varying step-out frequencies. Fig. 2(a) shows the scaled average microrobot angular velocity $\bar{\omega}_\mathrm{m}/\omega_\mathrm{so}$ of four hypothetical microrobots. The first microrobot (the "baseline") has a step-out frequency of ω_so and is the curve labeled A. The remaining three curves labeled B, C, and D show the scaled average angular velocity for three other microrobots whose step-out frequencies are scaled by a factor s (i.e., $s\omega_\mathrm{so}$) with $s = 2$, 3, and 4, respectively. The step-out frequency of the other microrobots could be scaled by increasing the microrobot's magnet volume by a factor of 2, 3, and 4, respectively.

The comparative effect of scaling a microrobot's step-out frequency is illustrated in Fig. 2(b), which shows the ratio $R(s)$ of each scaled microrobot's average rotation frequency to that of the baseline microrobot at the same frequency. For scaled field frequencies beneath the baseline step-out frequency $(\omega_\mathrm{h}/\omega_\mathrm{so} \leq 1)$, the ratio $R(s) = 1$. When the baseline microrobot reaches step-out, $R(s)$ increases. The maximum value of $R(s)$ occurs at the step-out frequency of the scaled microrobot, which produces

$$R_\mathrm{max}(s) = \frac{1}{1 - \sqrt{1 - (1/s)^2}} \underset{s\to\infty}{=} 2s^2. \tag{6}$$

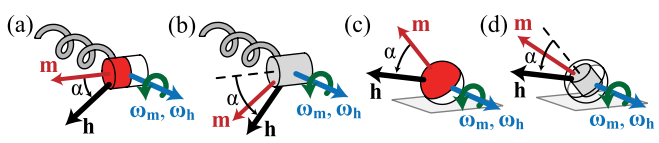

FIG. 1. This figure illustrates the 1-DOF model used herein. For permanent-magnet microrobots [(a) and (c)], α measures the angle between the applied field $\mathbf{h}$ and the microrobot's dipole moment $\mathbf{m}$. For soft-magnetic microrobots [(b) and (d)], α measures the angle between the applied field $\mathbf{h}$ and the major axis of the magnetic body.

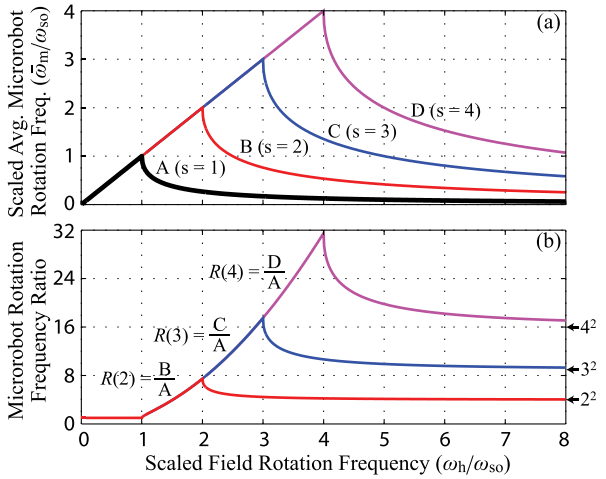

FIG. 2. (a) The scaled average microrobot rotation frequency $\bar{\omega}_\mathrm{m}/\omega_\mathrm{so}$ for four hypothetical microrobots as a function of the scaled field rotation frequency $\omega_\mathrm{h}/\omega_\mathrm{so}$, where ω_so is the step-out frequency of the "baseline" microrobot (with $s = 1$ and labeled A). The plots labeled B, C, and D are for three microrobots with the step-out frequency scaled from the baseline by factors $s = 2$, 3, and 4, respectively. (b) The ratio $R(s)$ of the scaled average microrobot rotation frequencies.

The maximum of $R(s)$ could be useful in the context of multi-microrobot control if it is desired that two sets of microrobots (denoted as set $\mathcal{A}$ and $\mathcal{B}$) have the ability to alternate between a mode where all microrobots rotate at the same frequency, and a mode where set $\mathcal{A}$ rotates a factor of $R_{\max}$ faster than set $\mathcal{B}$, selected by the magnetic field rotation frequency. In this example, the smallest factor s that the step-out frequency of the microrobots in set $\mathcal{A}$ should be scaled to achieve a desired maximum ratio $R_{\max}$ can be found by solving (6). The minimum factor s to achieve a desired $R_{\max}$ is $s \approx \sqrt{R_{\max}/2}$. Note that $R(s)$ ranges from 1 to $\sim 2s^2$ when the field rotation frequencies ranges between the baseline and scaled microrobot's step-out frequencies.

As the magnetic field rotation frequency increases past the scaled microrobot's step-out frequency, the ratio $R(s)$ drops and approaches a horizontal asymptote [see Fig. 2(b)]. In this regime, $R(s)$ is given by

$$R(s) = \frac{1 - \sqrt{1 - (s\omega_{so}/\omega_h)^2}}{1 - \sqrt{1 - (\omega_{so}/\omega_h)^2}} \underset{\omega_h \to \infty}{=} s^2. \quad (7)$$

In the context of controlling multiple sets of microrobots, the fact that $R(s)$ approaches a horizontal asymptote when both sets have lost field synchronization creates the possibility for complex control methods. For example, if there are three sets of microrobots denoted by $\mathcal{A}$, $\mathcal{B}$, and $\mathcal{C}$ with step-out frequencies scaled by factors $s = 1$, 2, and 3, respectively, then the ratios of their angular velocities can take on many combinations [refer to Fig. 2(b)]. For example, if the field is rotated at a scaled frequency in the range of [2.5, 3], then the ratio of set $\mathcal{B}$ and $\mathcal{A}$ velocities remains approximately constant near 4, while the ratio of set $\mathcal{C}$ and $\mathcal{A}$ velocities can range from approximately 12 to 18. Many combinations are possible, however a microrobot cannot rotate faster than another with a higher step-out frequency, provided the field rotates at a constant angular velocity. Additional selection can be achieved by designing groups to convert the rotating field to spatial velocity at different rates.

Fig. 3(a) shows the average microrobot rotation frequency $\bar{\omega}_m$ (left axis) and the corresponding average forward velocity (right axis) for the soft-magnetic helical swimmer[10] (shown in the inset) with two magnetizations resulting from the application of a 2 mT and 4 mT field, obtained while swimming in Methyl cellulose (0.2% w/v) near a silicon surface within a triaxial Helmholtz-coil system, which applies negligible magnetic forces. The average rotation frequency is deduced from measured forward velocity by recognizing that the microrobot and field rotation frequencies are the same below step-out (i.e., the slope of the average microrobot rotation frequency, plotted as a function of field rotation frequency, is 1 below step-out). A least-squares fit of (5) to each dataset is also shown. The step-out frequencies of the swimmer magnetized with the 2 mT (the "baseline") and 4 mT fields are 17.7 Hz and 23.9 Hz, respectively, indicating a scaling factor of $s = 1.35$. The ratio of the average microrobot rotation frequencies is plotted in Fig. 3(b), which falls in the range of [1.0, 3.0] for $\omega_h \in [17.7\,\text{Hz}, 23.9\,\text{Hz}]$, and approaches the horizontal asymptote $1.35^2 = 1.82$.

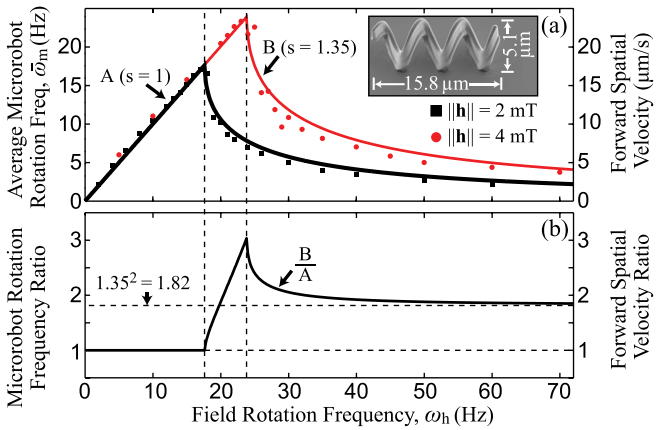

FIG. 3. (a) The average microrobot rotation frequency $\bar{\omega}_m$ for a soft-magnetic helical swimmer [shown in the inset] magnetized by a 2 mT and 4 mT magnitude field, as a function of field rotation frequency ω_h. The "baseline" swimmer ($s = 1$) is magnetized by the 2 mT magnitude field. The right axis denotes the swimmer's forward spatial velocity. The numerical similarity between the left and right axes is coincidental. (b) The ratio of the average microrobot rotation frequencies at both magnetizations. The right axis denotes the ratio of the forward spatial velocities.

Fig. 4(a) shows the average rotation frequency $\bar{\omega}_m$ for two permanent-magnet "microrobot" devices [one is shown in the inset of Fig. 4(a)], obtained from measured average device forward velocity in the same manner as Fig. 3(a), with $\|\mathbf{h}\| = 8$ mT. Each permanent-magnet "microrobot" device consists of a 2.55 mm diameter, 3.18 mm tall cylinder with an axially magnetized 1.59 mm diameter, 1.59 mm tall cylindrical NdFeB magnet positioned in the device's geometric center and polarized perpendicular to the device's longitudinal axis. Both devices are geometrically identical, but one contains an N52-grade magnet and the other contains an N42-grade magnet. The devices are actuated in a triaxial Helmholtz-coil system and roll on a polystyrene surface immersed in corn syrup with viscosity and density of 2500 cps and 1.36 g/ml, respectively. Reynolds-number analysis

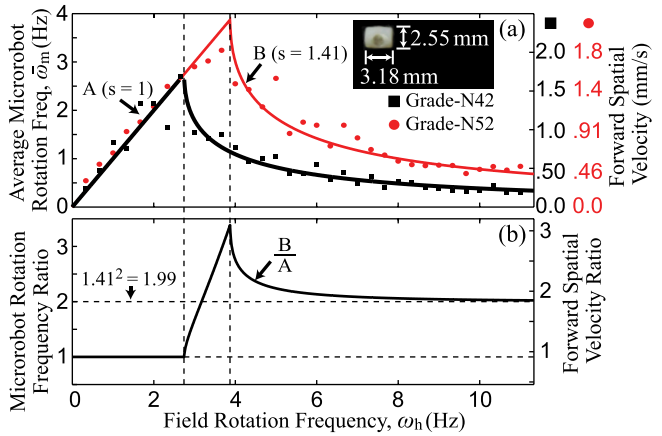

FIG. 4. (a) The average rotation frequency $\bar{\omega}_m$ is shown for two permanent-magnet rolling "microrobot" devices of the same geometry [see the inset of (a)], but one contains a N42-grade magnet and the other a N52-grade magnet, and with $\|\mathbf{h}\| = 8$ mT as a function of field rotation frequency ω_h. The right axes denote the devices' spatial velocities. (b) The ratio of the average device rotation frequencies. The right axis denotes the ratio of the devices' spatial velocities. Reynolds-number analysis predicts that both "microrobot" devices behave equivalently to a 60 μm diameter microrobot in water.

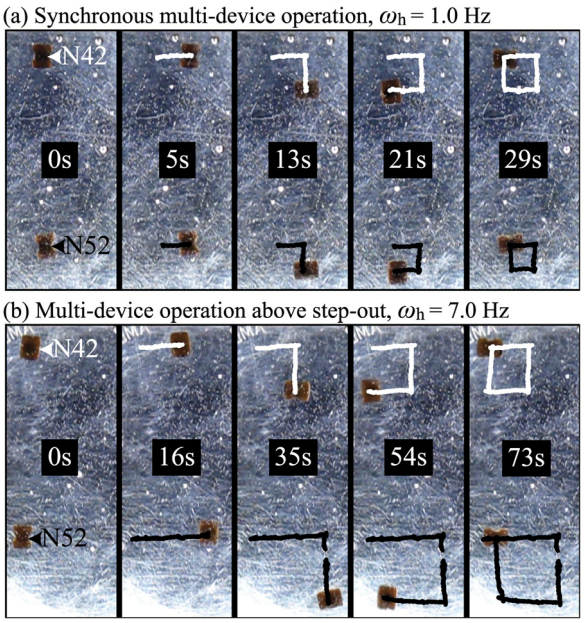

FIG. 5. A demonstration of selective control over the forward velocity ratio of two permanent-magnet "microrobot" devices by varying the field rotation frequency ω_h. In (a), both devices follow a square path with $\|\mathbf{h}\| = 8.0$ mT and $\omega_h = 1$ Hz, which is *below* both devices' step-out frequencies. The measured forward velocity ratio is 0.80. In (b), both devices follow a square path with $\|\mathbf{h}\| = 8.0$ mT and $\omega_h = 7$ Hz, which is *above* both devices' step-out frequencies. The measured forward velocity ratio is 1.7. (Multimedia view) [URL: http://dx.doi.org/10.1063/1.4870768.1]

predicts the behavior of both devices to be equivalent to a 60 μm diameter microrobot in water.

Although both "microrobot" devices are geometrically the same, unintended surface irregularities cause the forward velocity of the N42-grade device to be 9.9% faster than the N52-grade device for the same rotating frequencies. The step-out frequencies of the N42-grade (i.e., the "baseline") and N52-grade devices are 2.75 Hz and 3.88 Hz, respectively, which indicates a scaling factor of $s = 1.41$. Fig. 4(b) shows the ratio of the average device rotation frequencies, which falls in the range of [1.0, 3.38] for $\omega_h \in [2.75\,\text{Hz}, 3.88\,\text{Hz}]$, and approaches the horizontal asymptote $1.41^2 = 1.99$. The average forward velocity ratio approaches the horizontal asymptote 1.8.

Fig. 5 (with associated multimedia) demonstrates the use of the step-out behavior described herein for the simultaneous control of the two "microrobot" devices used in Fig. 4. Fig. 5(a) shows both devices actuated along a square path by driving the devices forward for 5 s, turning the devices $\pi/2$ rad clockwise over 3 s, and repeating until a square has been completed. The field rotates at 1 Hz, where both "microrobot" devices synchronously rotate, and $\|\mathbf{h}\| = 8.0$ mT. The N42- and N52-grade devices follow 4.4 mm and 3.4 mm square paths and travel at 0.88 mm/s and 0.68 mm/s, respectively, indicating a forward velocity ratio of 0.80 (Fig. 4(b) predicts 0.91).

Fig. 5(b) shows both permanent-magnet "microrobot" devices operated with $\|\mathbf{h}\| = 8.0$ mT and $\omega_h = 7$ Hz, which is above both devices' step-out frequencies. In this case, the path is generated by driving the devices for 16 s and turning for 3 s. The N42- and N52-grade "microrobot" devices follow 5.1 mm and 8.8 mm square paths and travel at 0.32 mm/s and 0.55 mm/s, respectively, indicating a forward velocity ratio of 1.7 (Fig. 4(b) predicts 1.8). This demonstrates the ability to selectively control the ratio of the microrobots' forward velocities by operating both devices above their step-out frequencies.

The analysis presented herein can add an additional level of microrobot differentiation to existing multi-microrobot control methods (e.g., addressable actuation strategies that have proven useful for positioning and manipulation[2]), and may be applied to exploit natural variance in batch-manufactured microrobots for the control of microrobot swarms. This work was partially funded by the National Science Foundation under Grant No. 0952718 and European Research Council Advanced Grant BOTMED.

[1]B. J. Nelson, I. K. Kaliakatsos, and J. J. Abbott, Annu. Rev. Biomed. Eng. **12**, 55 (2010).
[2]E. Diller and M. Sitti, Found. Trends Rob. **2**, 143 (2013).
[3]K. Ishiyama, M. Sendoh, and K. I. Arai, J. Magn. Magn. Mater. **242–245**, 41 (2002).
[4]T. Bretl, IEEE Trans. Robot. **28**, 351 (2012).
[5]J. J. Abbott, O. Ergeneman, M. P. Kummer, A. M. Hirt, and B. J. Nelson, IEEE Trans. Rob. **23**, 1247 (2007).
[6]B. H. McNaughton, K. A. Kehbien, J. N. Anker, and R. Kopelman, J. Phys. Chem. B **110**, 18958 (2006).
[7]A. Ghosh, P. Mandal, S. Karmakar, and A. Ghosh, Phys. Chem. Chem. Phys. **15**, 10817 (2013).
[8]V. M. Fomin, E. J. Smith, D. Makarov, S. Sanchez, and O. G. Schmidt, Phys. Rev. B **84**, 174303 (2011).
[9]P. Tierno, J. Claret, F. Sagues, and A. Cebers, Phys. Rev. E **79**, 021501 (2009).
[10]S. Tottori, L. Zhang, F. Qiu, K. K. Krawczyk, A. Franco-Obregón, and B. J. Nelson, Adv. Mater. **24**, 811 (2012).